Case Studies in Thermal Engineering 23 (2021) 100812

Contents lists available at ScienceDirect

Case Studies in Thermal Engineering

journal homepage: http://www.elsevier.com/locate/csite

Insights from bond-slip investigations in different reinforced concrete mixtures for LNG containment

Reginald B. Kogbara [a,*], Myungjin Seong [b], Dan G. Zollinger [b], Srinath R. Iyengar [a], Zachary C. Grasley [b], Eyad A. Masad [a,b]

[a] Mechanical Engineering Program, Texas A&M University at Qatar, P.O. 23874, Education City, Doha, Qatar
[b] Zachry Department of Civil & Environmental Engineering, Texas A&M University, College Station, TX, 77843, USA

ARTICLE INFO

Keywords:
Air entrainment
Cryogenic steel
Cryogenic temperatures
Internal strain
Pull-out testing
Vibrating wire gages

ABSTRACT

Understanding the concrete-steel interface's behavior at cryogenic temperatures is important for designing concrete for direct liquefied natural gas (LNG) containment; such behavior is currently unclear. Hence, the work conducted involved pull-out testing in providing insights on the bond-slip relationship and the development of internal strains, which have seldom been measured in cryogenic concrete. Deformed cryogenic steel rebars (16 and 19 mm diameter) were embedded in cylindrical concrete specimens made with either traprock or limestone aggregates, with and without air entrainment (AE). Embedded foil and vibrating wire gages monitored the concrete and rebar's internal strains during cooling and pull-out testing. Pull-out testing involving applied stresses ranging from 34.5 to 241.5 MPa was conducted at normal and cryogenic temperatures. Bond stress was similar in both aggregate types but increased with rebar diameter within the applied stress range. The gages indicated that the rebar and concrete showed similar strain patterns in AE and non-AE traprock, and the AE limestone concretes during cryogenic cooling. However, the rebar gages responded to expansive movements below −20 °C in the non-AE limestone concrete. Bond stiffness degradation occurred at higher applied tensile stresses with AE in limestone concrete but at similar tensile stresses in AE and non-AE traprock concrete.

1. Introduction

The primary containment tank for liquefied natural gas (LNG) storage is conventionally made with 9% Ni steel, which is becoming increasingly expensive. Hence, there is increased attention towards usage of concrete for direct LNG containment since concrete properties generally improve at cryogenic temperatures [1]. More recent studies on cryogenic concrete behavior have focused on mechanical, thermal and pore structure properties of plain concrete [2–7]. Studies on reinforced concrete at cryogenic temperatures have focused on the bond strength to reinforcement alongside tensile strength, and mechanical properties of steel reinforcement such as yield and ultimate strengths [8,9]. The bond strength at cryogenic temperatures was reported to be about six times that at ambient temperature for air-entrained (AE) concrete, and two to three times for non-AE concrete [10]. It is influenced by moisture content and aggregate type [1].

The different coefficients of thermal expansion (CTEs) of concrete and steel make their interaction (bond-slip) forces different [7]. Nevertheless, very few studies have considered the stresses and strains in both materials simultaneously in reinforced concrete during

* Corresponding author.
E-mail address: reginald.kogbara@qatar.tamu.edu (R.B. Kogbara).

https://doi.org/10.1016/j.csite.2020.100812
Received 29 June 2020; Received in revised form 7 December 2020; Accepted 11 December 2020
Available online 15 December 2020

cryogenic cooling and pull-out testing. Previous studies mostly focused on the thermal behavior of each material separately [1,9,11]. The thermal deformation behavior of reinforcing steel and oven-dried concrete is almost linear with temperature decrease. In contrast, that of water-saturated concrete includes an expansion phase in the −10 to −60 °C temperature range [11]. Thus, these differences may cause internal stresses such that the steel may be overstressed while the concrete may suffer an additional compression [11].

Substantial temperature changes result in thermal stresses on the reinforcement and surrounding concrete, and associated strains. Hence, this study sought to investigate the internal strains developed in the rebar and concrete in reinforced concrete specimens subjected to cryogenic temperatures as they relate to the development of the bond between steel and concrete. The effect of these internal strains during cryogenic cooling on bond behavior is not well documented. Furthermore, the use of vibrating wire (VW) gages employed in this work for strain measurement in cryogenic concrete is rare in the literature. Therefore, this study aimed to examine the dependence of the internal strains and bond behavior (stress and stiffness) on different parameters such as aggregate type, air entrainment, and rebar size.

2. Experimental methodology

2.1. Concrete mixture design

The concrete mixtures were designed to exceed the 34.5 MPa minimum compressive strength [12] specified for containment of refrigerated liquefied gases following ASTM C 192 [13]. River sand was used as the fine aggregate, while traprock and limestone were used as coarse aggregates. A set of AE mixtures with 6% air content were tested only at cryogenic temperatures since AE is usually required for frost protection. Table 1 shows the concrete mixture parameters.

2.2. Strain gage installation and concrete specimen preparation

Foil strain gages, CFLA-6-350-11-6FA3LT (*TML*, Japan), and specially designed cryogenic-rated 4200X model VW strain gages (*Geokon Inc.*, New Hampshire, USA) were employed as rebar and concrete gages, respectively. Each VW gage also incorporates a thermistor for temperature measurement. Deformed cryogenic steel (CryoSTEEL®) rebars (*CMC Steel*, Arizona, USA) with 16- and 19-mm diameters and 750 mm long, were employed. Unlike classical steel rebars that tend to become brittle with temperature reduction, cryogenic steel retains suitable engineering properties such as yield, tensile strength and ductility at cryogenic temperatures. In contrast to cryogenic steel, if standard steel rebar is used as reinforcement, the concrete will crack. The specified minimum tensile and yield strengths of the rebars used are 620 and 500 MPa, respectively, at room temperature and there is an increase in these properties as the temperature decreases as well. The rebars employed are specified to have a minimum of 12% elongation (an indication of good ductility) in 8 inches (200 mm) at ambient temperature and 3% at cryogenic design temperature (−170 °C).

The foil gages were fixed into slots made on the surface of the rebar using cyanoacrylate (CN) adhesive (*TML*, Japan), and covered with K-1 coating material – a special white rubber for moisture proofing (*TML*, Japan). The CN adhesive has an operating temperature range of −196 to 120 °C and has been proven to maintain a durable bond with foil strain gages at cryogenic temperatures [14]. Metal sheaths with hexagonal flanges were placed over the VW gage flanges such that the sheaths' flanges anchor at 62.5 mm in order to reduce the effective length of the gages from 150 mm (Fig. 1a and c). A compressible (rubber) material was placed at the other end of the metal sheath to allow for expansion. The gage modification enabled better capturing of the strain gradient, which is of a large magnitude, and did not affect the functionality of the internal vibrating wire.

Two sets of foil and VW gages were used in a given concrete specimen. Both gage types were placed side by side on opposite sides of the rebar (Fig. 1c). The gages were installed such that the center of both gage types was at ~56 and 119 mm from the top surface of the concrete specimen (Fig. 1a). The gages were placed within the upper half of the concrete specimen since the maximum local bond stress moves toward the loaded end with increase in load, and the bond stress is minimal in the lower half [15]. The instrumented rebar was positioned in a 150 mm diameter by 300 mm long mold (Fig. 1d), a Type T thermocouple for internal temperature measurement placed slightly below the center of the specimen (Fig. 1a), and the concrete specimen cast. After casting, sealed curing was conducted for 48 h and the specimen demolded thereafter. The specimen was then cured at a temperature of 20 °C and 50% relative humidity for 28 days.

Table 1
Concrete mixture design and specimen properties.

Constituent/property	Non-AE traprock	Non-AE limestone	AE traprock	AE limestone
Cement (kg/m^3)	338	338	338	338
Coarse aggregate (kg/m^3)	1172	1091	1172	1091
Fine aggregate (kg/m^3)	432	720	432	720
Water (kg/m^3)	168	168	168	168
MasterAir AE 200[a] (kg/m^3)	–	–	0.71	0.44
Bulk density[b] (kg/m^3)	2438	2396	2328	2366
Compressive strength[b] (kg/m^3)	40	37	42	34.5

AE – Air entrained.
[a] Air-entraining admixture (from *BASF*, Ohio).
[b] Tested at 28 days on 75 mm diameter cylinders.

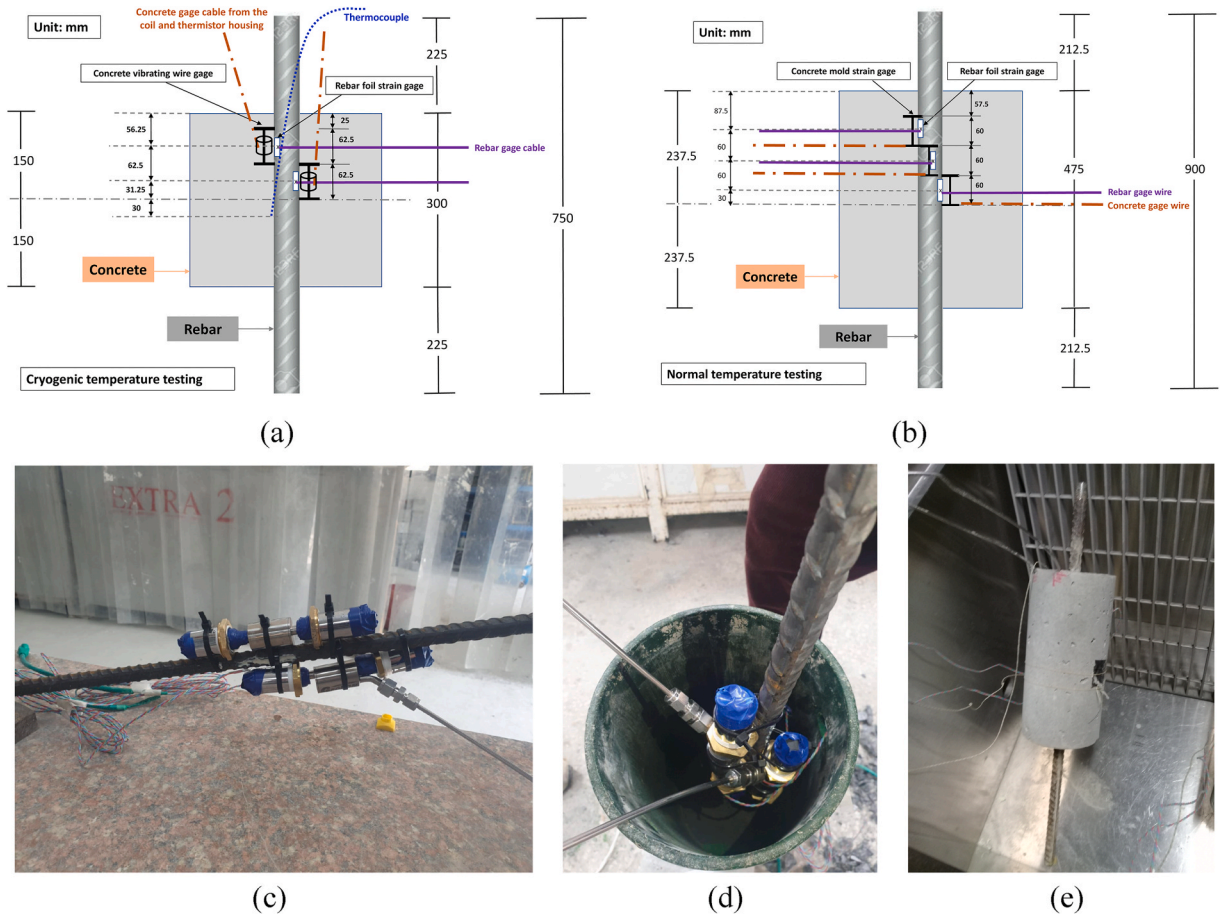

Fig. 1. Experimental set-up indicating schematic of the precise location of the gages in specimens for (a) cryogenic temperature testing, and (b) normal temperature testing, and photos showing (c) arrangement of the strain gages on rebar, (d) placement of the instrumented rebar in a concrete mold, and (e) reinforced concrete specimen in the temperature chamber.

The above describes the materials/equipment used for the main testing at cryogenic temperatures. For some reasons, including testing conditions and cost, there were slight differences in some items used for testing at normal temperatures. Thus, FLA-5-11-5LJC foil strain gages and PMFL-60-2LJRTA mold strain gages (with 60 mm gage length) from *TML*, Japan, were used as rebar and concrete gages, respectively. Further, a 475 mm long concrete specimen with the same diameter above was used together with a 900 mm cryogenic steel rebar. These accommodated three sets of foil and VW gages, with the center of the gages placed at 87.5, 147.5 and 207.5 mm from the top surface of the concrete specimen (Fig. 1b).

2.3. Cryogenic cooling and pull-out testing

Concrete specimens were cooled in a temperature chamber (*CSZ*, Ohio, USA) (Fig. 2a) using a single set point with ~3 °C/min cooling rate. The specimens were cooled to around −180 °C, as indicated by a data logger (*Supco*, New Jersey, USA) connected to the inserted thermocouple. Albeit, the temperature values reported in the results section were the averages of the data from the thermocouple and temperatures recorded by the thermistors of the VW gages. Thus, the temperature data was taken from three different points inside a specimen (see Fig. 1a) to allow for thermal diffusion effects since the temperature field is not homogenous during cooling. The frozen specimen was then stored in a Corafoam® thermal insulation material (i.e., rigid polyisocyanurate foams, *Duna Corradini*, Modena, Italy) (Fig. 2a) and transferred for pull-out testing (Fig. 2b).

The strains in the rebar and concrete were recorded by portable D4 (*VPG, Inc.,* USA) and LC-2 (*Geokon Inc.*, New Hampshire, USA) data loggers, respectively, during cryogenic cooling and pull-out testing. The actual strains of the foil gages during cryogenic cooling were determined from algebraic compensation of the recorded thermal output (apparent) strains previously described elsewhere [14]. Similarly, the actual strains undergone by the concrete was obtained from temperature correction of the VW gages apparent strain output following the procedure in the Geokon strain gage manual. Actual strain determination was based on temperature data from the thermistors. Information on the apparent strain output or behavior of the foil and VW gages during cryogenic cooling when not bonded to a rebar or embedded in concrete is shown in Fig. 2c.

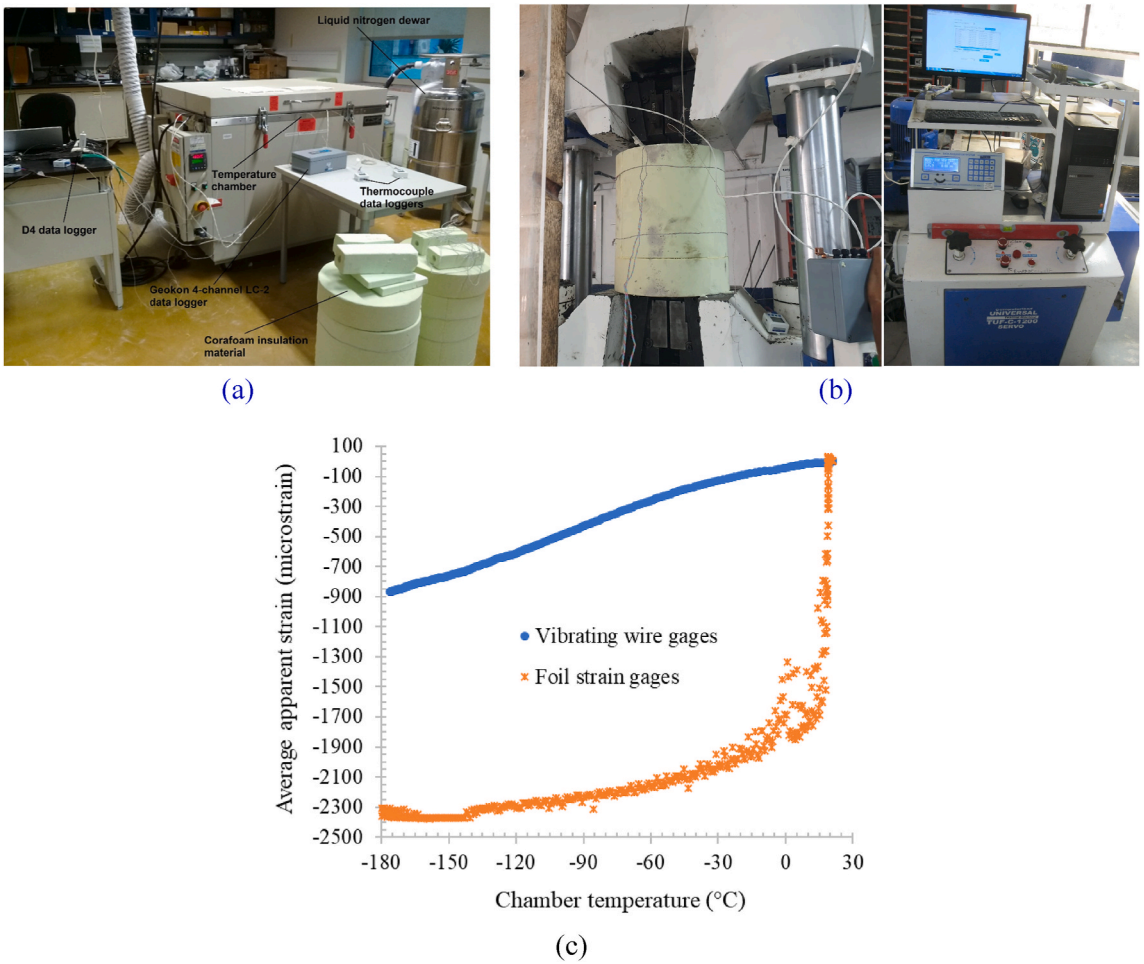

Fig. 2. Experimental photographs showing the (a) cryogenic cooling process in the LN2-cooled temperature chamber, data loggers, and insulation material, and (b) set up during pull-out testing of cryogenically frozen concrete specimen, and (c) functional test data showing the average apparent strain behavior of the foil and VW gages with cryogenic cooling when not embedded in concrete.

Specimens for pull-out testing at normal temperatures were not subjected to the above cooling process. The frozen specimens were kept in the coraform insulation material during the pull-out tests to minimize heat gain (Fig. 2b). The temperature rises during the pull-out testing were, on average 6 °C. A Servo Computerized Universal Testing Machine TUF-C-1200 was employed for the pull-out testing with an average loading rate of 0.81 kN/s. Seven stress levels (34.5, 69, 103.5, 138, 172.5, 207 and 241.5 MPa) were applied on a given specimen during pull-out testing. The specimen was loaded to a given stress level, unloaded to 0 MPa, and reloaded to the next stress level in succession and the load values and internal strains at each stress level recorded.

3. Results and discussion

3.1. Bond stress and stiffness

The bond stress at a given applied tensile stress was determined according to Equation (1):

$$\tau_b = \frac{F}{\pi \times d_s \times l_s} \tag{1}$$

Where, τ_b is the bond stress, F is the applied tensile force, $d_s$is the rebar diameter, and l_s is the embedment length of the rebar.

The bond stiffness was determined as the slope of the bond stress versus rebar strain curve for a given applied tensile stress. The bond stress increased with the applied tensile stress at both normal and cryogenic temperatures (Fig. 3a and c). It was similar in the traprock and limestone mixtures at normal and cryogenic temperatures since it was determined using Equation (1), and the applied stress levels and rebar diameters were identical for both aggregates. Any slight differences in bond stress that are observed between the concrete mixtures in Fig. 3a and c are due to small differences in the pull-out machine's output load values during testing. On average,

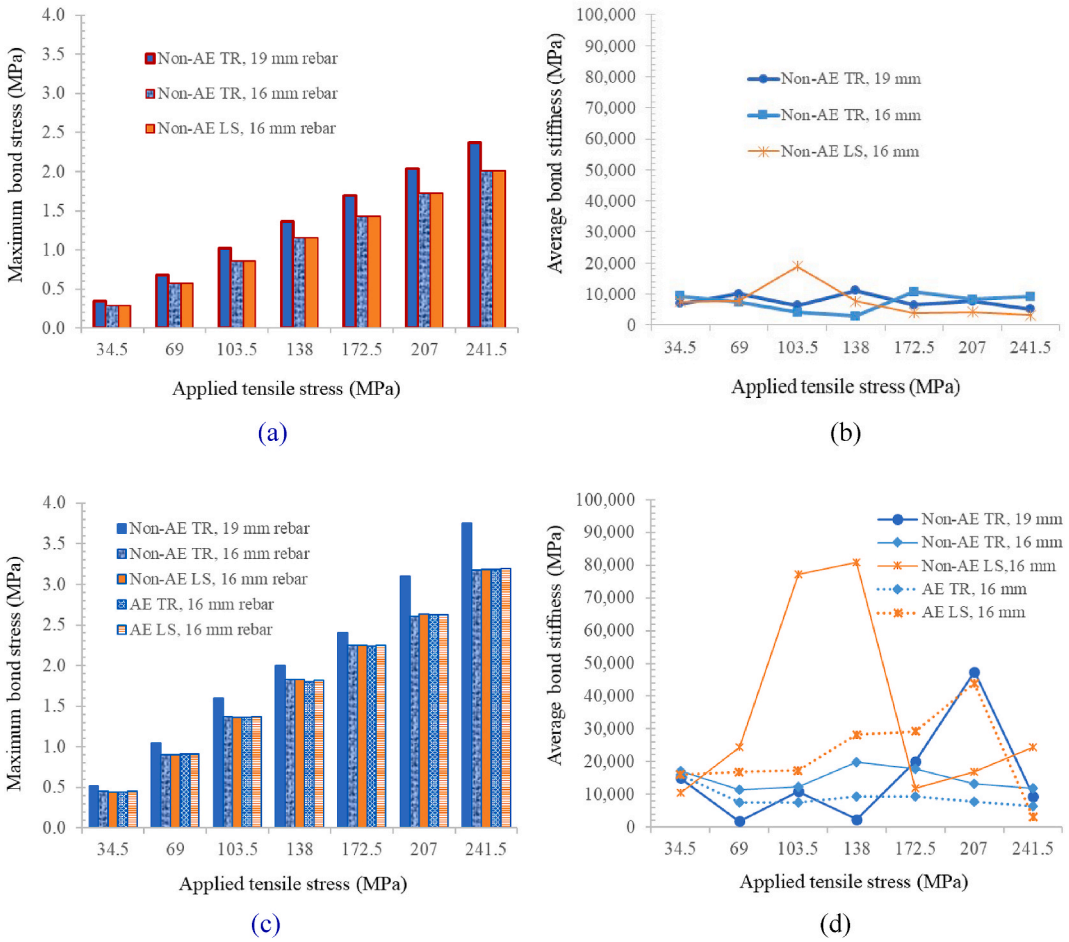

Fig. 3. Maximum bond stress and average bond stiffness in different concrete specimens at (a) & (b) normal temperature, and (c) & (d) cryogenic temperatures, respectively. *Note: AE – Air-entrained, TR – Traprock, LS – Limestone. The data for bond stress and stiffness are the averages of the gages used. The embedment length was different for normal and cryogenic temperature specimens (see Fig. 1). Hence, the difference in bond stresses.*

the bond stress was about 52–57% higher at cryogenic (~1.8 MPa) than at normal (~1.2 MPa) temperature. However, as noted previously, the normal temperature specimens had longer embedment lengths than the cryogenic temperature specimens (see Fig. 1). With embedment length in the denominator of Equation (1), the above will lead to lower bond stresses in the former (Fig. 3a) than the latter (Fig. 3c). There was a roughly 15% increase in bond stress with the 19 mm rebar compared to the 16 mm rebar in the traprock mixture, where the rebar size effect was evaluated. This differs from the findings of previous studies [16] in which the bond strength of deformed bars decreases with increasing rebar diameter. The difference is due to the limitation of the applied stress range such that the specimen was not pulled to failure; hence, the applied tensile force was lesser in the lower diameter rebar.

The average bond stiffness values at cryogenic temperatures were roughly double those at normal temperatures (Fig. 3b and d). The stiffness was similar at normal temperatures, but a lot higher for the limestone than traprock mixture at cryogenic temperatures. Bond stiffness reduced with AE in mixtures with both aggregates at cryogenic temperatures (Fig. 3d). This reduction could be due to the reduced capacity of the cement paste to form a strong contact layer along the bonded interface due to the presence of large numbers of air bubbles [17]. Although bond stiffness reduced with AE, the stiffness trend with increasing applied tensile stress sheds some light on the bond behavior. Several factors including yielding of reinforcement and bond slip could lead to loss of stiffness [18]. An abrupt loss of stiffness occurred at applied stresses of 172.5 and 241.5 MPa for the non-AE and AE limestone specimens, respectively, suggesting better bond behavior with AE (Fig. 3d). In contrast, AE made no difference in the traprock mixtures as bond stiffness degraded less abruptly in the 16 mm rebar specimens around 172.5–207 MPa stress (Fig. 3d).

3.2. Internal strains in rebar and concrete

The maximum strains in the rebar and concrete during pull-out testing at normal and cryogenic temperatures alongside the actual strains during cryogenic cooling are shown in Fig. 4. The recorded strains are presented as the averages of the two or three gages in a specimen since this is a short communication article. This corresponds to the specimen's average temperature data obtained from the

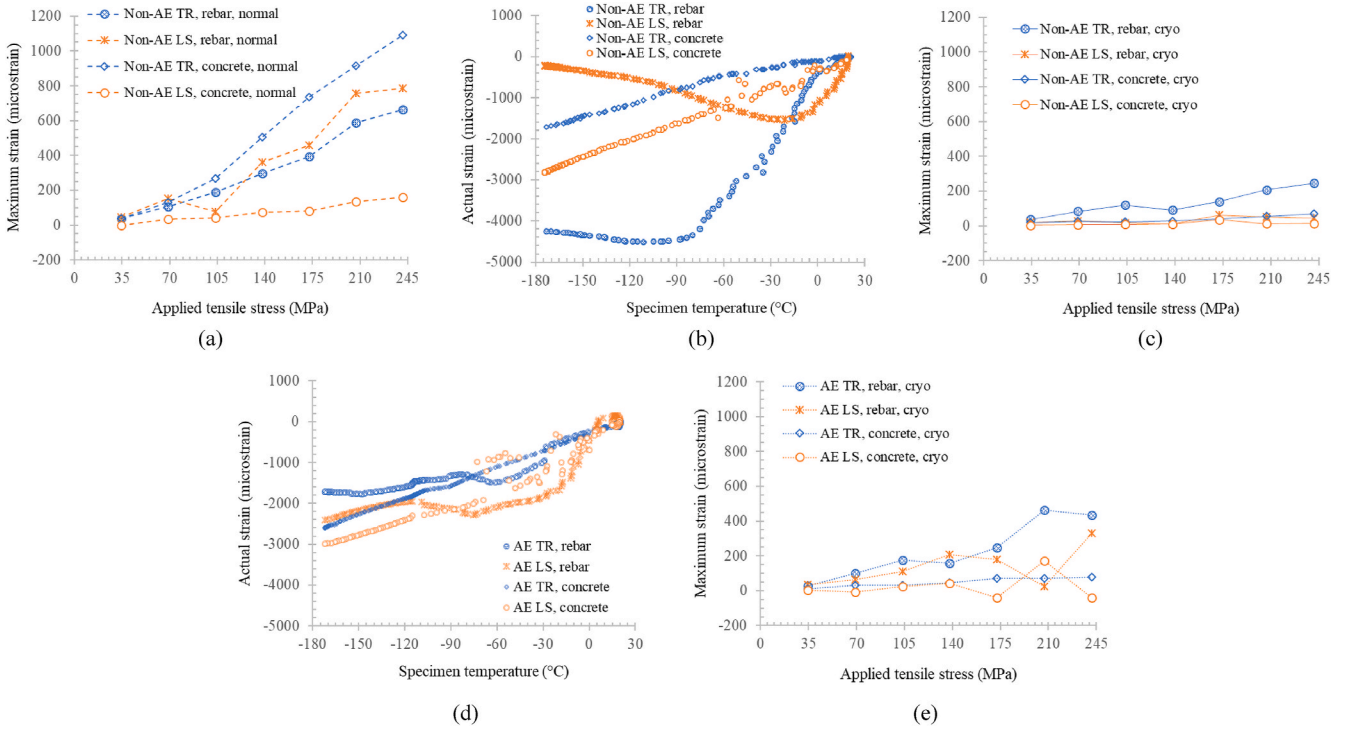

Fig. 4. Maximum and actual strains in concrete mixtures due to, (a) pull-out testing at normal temperature, (b) cryogenic cooling, and (c) pull-out testing at cryogenic temperatures, for non-air-entrained mixtures, (d) cryogenic cooling, and (e) pull-out testing at cryogenic temperatures, for air-entrained mixtures. *Note: AE – Air-entrained, TR – Traprock, LS – Limestone, cryo – cryogenic.*

VW gages' thermistors and inserted thermocouple, as mentioned previously. Hence, the strain profile evolution with temperature for the different gages along the embedment length, modeling residual strains and temperature fields in the specimens, and crack width analysis is beyond this paper's scope and will be treated in a separate publication.

The maximum strains during pull-out testing were a lot higher at normal than cryogenic temperatures (Fig. 4a and c), especially in the limestone mixtures. This points to a reduction in ductility of the materials with cryogenic cooling [7]. As noted previously, the bond stresses were similar for AE and non-AE specimens with both aggregates. Thus, the higher strains in the AE specimens (Fig. 4e) compared to the non-AE specimens (Fig. 4c) suggest that AE improves the ductility and toughness (area under a stress-strain curve) of the specimens at cryogenic temperatures. Similarly, the traprock specimens with higher strains are likely to be less brittle and tougher than the limestone mixtures.

The strain behavior during cryogenic cooling generally indicated contraction in the concrete and rebar. The strain trend in both materials appeared to move together, displaying little differences (Fig. 4b and d). However, below −20 °C, the rebar gages in the non-AE limestone mixture responded to expansive movements in the concrete, which showed the previously mentioned complex strain behavior in the 0 to – 60 °C temperature range (Fig. 4b). The dissimilar strain behavior of the embedded rebar is likely to produce additional compression and cracking damage in the specimen. It could also cause significant residual stresses in the specimen before pull-out testing. The apparent expansion in some of the specimens as they approached the lowest temperatures is due to decreased LN2 injection after the temperature chamber stabilized at −180 °C. The use of AE in the limestone mixture prevented the embedded rebar from responding to expansive movements. The AE limestone concrete expanded in the −20 to −70 °C range but it exhibited a similar strain pattern to the rebar (Fig. 4d). AE also reduced the strain difference between rebar and concrete in the traprock mixture. These observations suggest that substantial residual stresses present in the limestone specimens before pull-out testing might contribute to the aforementioned abrupt bond stiffness loss.

The effect of rebar size in the traprock mixtures on the internal strains was not straight forward (Fig. 5). The concrete and rebar showed higher strains in the specimen with a 16 mm rebar than that with a 19 mm rebar at normal temperatures. However, the opposite occurred at cryogenic temperatures (Fig. 5a and b). The concrete specimen with a 19 mm rebar had more strain, although its

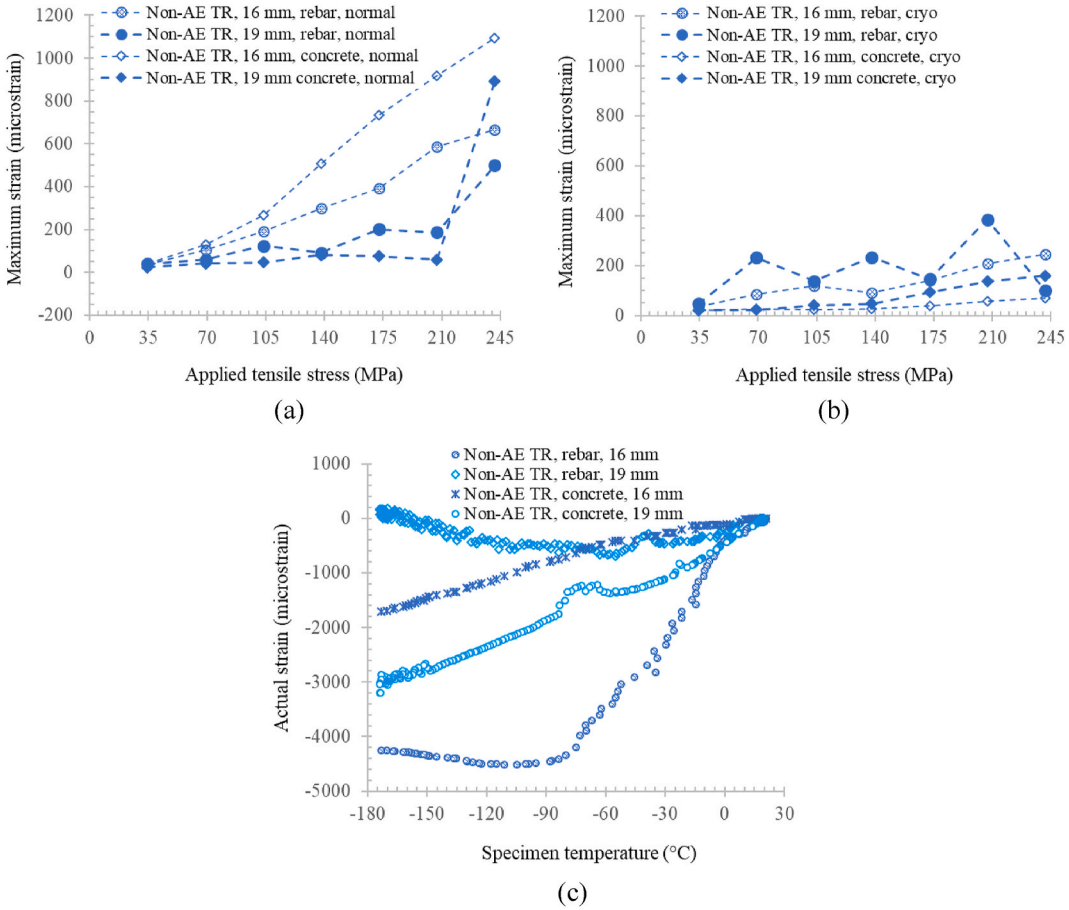

Fig. 5. The effect of rebar diameter on maximum and actual strains in concrete specimens made with traprock aggregate due to (a) & (b) pull-out testing at normal and cryogenic temperatures, respectively, and (c) cryogenic cooling. *Note: AE – Air-entrained, TR – Traprock, LS – Limestone, cryo – cryogenic. The effect of rebar size was not investigated in the limestone mixtures.*

rebar showed lesser strain than its 16 mm rebar counterpart during cryogenic cooling (Fig. 5c). On average, the bond stiffness of the 19 mm specimen was slightly higher than those of the 16 mm specimen. Hence, there may be no significant advantage of using the 19 mm over the 16 mm rebar.

Furthermore, work is in progress to evaluate any possible deleterious effect of cryogenic freeze-thaw cycling on residual stresses and bond stiffness degradation in the concrete mixtures. Nevertheless, freeze-thaw cycling is not typically a problem for concrete LNG containment tanks since the primary tank never undergoes full cryogenic freeze-thaw cycles. LNG storage tank systems are usually in continuous operation. The tank never goes empty once filled with LNG, except for a receiving terminal tank that is continuously filled and emptied [1,3].

4. Conclusions

This study's findings demonstrated that expansive movements during cryogenic cooling cause more pronounced dissimilar strain behavior between concrete and rebar in reinforced concrete specimens made with limestone than traprock aggregate. The difference in the strain trend with decreasing temperatures between non-AE limestone concrete and its embedded rebar manifested in an abrupt loss of its higher bond stiffness at an applied tensile stress of 172.5 MPa. AE generally led to a similar strain trend between rebar and concrete during cryogenic cooling and higher tensile stress before bond stiffness loss in limestone concrete. However, AE had no noticeable impact on bond stiffness degradation in traprock concrete. These investigations may enhance understanding of the bond resistance mechanism in cryogenic concrete. Further studies will consider the strain profile evolution at each gage location with temperature in the concrete and rebar and model residual strains inside the reinforced concrete specimens. Such investigations will detail the effect of cryogenic temperatures on stress transfer and improve understanding of the measured concrete strain from thermal expansion. The effect of freeze-thaw cycling on possible bond stiffness degradation will also be considered.

Credit author statement

R.B. Kogbara: Conceptualization, Methodology, Investigation, Formal analysis, Writing - original draft. **M. Seong**: Methodology, Investigation, Formal analysis, Writing – review and editing. **D.G. Zollinger**: Conceptualization, Methodology, Supervision, Writing – review and editing. **S.R. Iyengar**: Conceptualization, Writing – review and editing. **Z.C. Grasley**: Conceptualization, Writing – review and editing. **E.A. Masad**: Supervision, Writing – review and editing.

Declaration of competing interest

The authors declare that they have no known competing financial interests or personal relationships that could have appeared to influence the work reported in this paper.

Acknowledgements

This publication was made possible by an NPRP award (NPRP No. 9-448-2-176: Constitutive modeling and investigation of bond-slip relationship in concrete for direct liquefied natural gas containment) from the Qatar National Research Fund (QNRF – a member of The Qatar Foundation). The statements made herein are solely the responsibility of the authors. The authors are thankful to CMC Steel, Arizona, and BASF, Ohio, for kindly providing the cryogenic steel rebars and the MasterAir AE 200 air entrainment agent, respectively. Open Access funding provided by the Qatar National Library.

References

[1] R.B. Kogbara, S.R. Iyengar, Z.C. Grasley, E.A. Masad, D.G. Zollinger, A review of concrete properties at cryogenic temperatures: towards direct LNG containment, Construct. Build. Mater. 47 (2013) 760–770.
[2] R.B. Kogbara, S.R. Iyengar, Z. Grasley, E.A. Masad, D.G. Zollinger, Non-destructive evaluation of concrete mixtures for direct LNG containment, Mater. Des. 82 (2015) 260–272.
[3] R.B. Kogbara, S.R. Iyengar, Z.C. Grasley, S. Rahman, E.A. Masad, D.G. Zollinger, Relating damage evolution of concrete cooled to cryogenic temperatures to permeability, Cryogenics 64 (2014) 21–28.
[4] Y. Wang, Y. Cao, P. Zhang, Y. Ma, T. Zhao, H. Wang, Z. Zhang, Water absorption and chloride diffusivity of concrete under the coupling effect of uniaxial compressive load and freeze–thaw cycles, Construct. Build. Mater. 209 (2019) 566–576.
[5] J. Zhengwu, D. Zilong, Z. Xinping, L. Wenting, Increased strength and related mechanisms for mortars at cryogenic temperatures, Cryogenics 94 (2018) 5–13.
[6] J. Xie, X. Chen, J.-B. Yan, G. Lei, L. Zhu, Ultimate strength behavior of prestressed concrete beams at cryogenic temperatures, Mater. Struct. 50 (2017) 81–94.
[7] Z. Jiang, B. He, X. Zhu, Q. Ren, Y. Zhang, State-of-the-art review on properties evolution and deterioration mechanism of concrete at cryogenic temperature, Construct. Build. Mater. 257 (2020), https://doi.org/10.1016/j.conbuildmat.2020.119456. Article number 119456, doi: 119410.111016/j.conbuildmat.112020.119456.
[8] M.-J. Kim, S. Kim, S.-K. Lee, J.-H. Kim, K. Lee, D.-Y. Yoo, Mechanical properties of ultra-high-performance fiber-reinforced concrete at cryogenic temperatures, Construct. Build. Mater. 157 (2017) 498–508.
[9] J.-B. Yan, J. Xie, Behaviours of reinforced concrete beams under low temperatures, Construct. Build. Mater. 141 (2017) 410–425.
[10] S. Yemane, H. Kasami, T. Okuno, Properties of concrete at very low temperatures, in: Douglas McHenry International Symposium on Concrete and Concrete Structures, vol. 55, American Concrete Institute Special publication, 1978, pp. 207–222.
[11] M. Elices, Cryogenic prestressed concrete: fracture aspects, Theor. Appl. Fract. Mech. 7 (1987) 51–63.
[12] ACI, 376-11: Code Requirements for Design and Construction of Concrete Structures for the Containment of Refrigerated Liquefied Gases and Commentary, American Concrete Institute, 2013.

[13] ASTM, ASTM C192/C192M-02, Standard Practice for Making and Curing Concrete Test Specimens in the Laboratory, ASTM International, West Conshohocken, PA, 2002.
[14] R.B. Kogbara, S.R. Iyengar, Z.C. Grasley, S. Rahman, E.A. Masad, D.G. Zollinger, Correlation between thermal deformation and microcracking in concrete during cryogenic cooling, NDT E Int. 77 (2016) 1–10.
[15] T.P. Tassios, E.G. Koroneos, Local bond-slip relationships by means of the Moire method, ACI J. Proc. 81 (1984) 27–34.
[16] P.F. Bamonte, P.G. Gambarova, High-bond bars in NSC and HPC: study on size effect and on the local bond stress-slip law, J. Struct. Eng. 133 (2007) 225–234.
[17] H.O. Sugo, A.W. Page, S.J. Lawrence, The influence of air entraining agent on bond strength and mortar microstructure, in: Proceedings of the 6th Australasian Masonry Conference, Adelaide, South Australia, 2001, pp. 357–362.
[18] M. Aschheim, E. Hernández-Montes, D. Vamvatsikos, Design of Reinforced Concrete Buildings for Seismic Performance: Practical Deterministic and Probabilistic Approaches, CRC Press, Boca Raton, FL, 2019.